JOURNAL OF COMPUTATIONAL PHYSICS **146,** 546–569 (1998)
ARTICLE NO. CP986027

A Taylor–Galerkin Method for Simulating Nonlinear Dispersive Water Waves

D. Ambrosi* and L. Quartapelle†

**Dipartimento di Matematica, Politecnico di Torino, corso Duca degli Abruzzi 24, 10129 Turin, Italy; and †Dipartimento di Fisica, Politecnico di Milano, piazza Leonardo da Vinci, 32, 20133 Milan, Italy*

Received November 19, 1996; revised May 12, 1998

A new numerical scheme for computing the evolution of water waves with a moderate curvature of the free surface, modeled by the dispersive shallow water equations, is described. The discretization of this system of equations is faced with two kinds of numerical difficulties: the nonsymmetric character of the (nonlinear) advection–propagation operator and the presence of third order mixed derivatives accounting for the dispersion phenomenon. In this paper it is shown that the Taylor–Galerkin finite element method can be used to discretize the problem, ensuring second order accuracy both in time and space and guaranteeing at the same time unconditional stability. The properties of the scheme are investigated by performing a numerical stability analysis of a linearized model of the scalar 1D regularized long wave equation. The proposed scheme extends straightforwardly to the fully nonlinear 2D system, which is solved here for the first time on arbitrary unstructured meshes. The results of the numerical simulation of a solitary wave overpassing a vertical circular cylinder are presented and discussed in a physical perspective.

Key Words: shallow water equations; nonlinear dispersive waves; Taylor–Galerkin method; finite elements.

1. INTRODUCTION

Since the celebrated Scott Russel's discovery in 1834 of the existence of solitary waves, a deeper and deeper mathematical understanding of the dynamics of nonlinear dispersive waves has been attained (for a historical overview see [1, 2]). Restricting the attention to systems of equations that admit two-way travelling waves, several dispersive shallow water equations have been proposed in the literature to describe the dynamics of finite amplitude dispersive water waves (see, for instance, [3–6]).

Dispersive shallow water systems (sometimes also referred to as Boussinesq-type systems) can be deduced by means of an asymptotic expansion technique, starting from the

0021-9991/98 $25.00

potential equation for irrotational motion and from appropriate boundary conditions at the free surface of the water. This derivation is based on two assumptions: fairly long waves and small elevation of the free surface with respect to depth [4, 7]. If the vertically averaged velocity is the unknown, the dispersive shallow water system so deduced differs from the nondispersive model by the occurrence of a third order mixed derivative term in the momentum equation. This term accounts for the dispersion, i.e., the propagation at different phase speeds of wave components of different wavelength and amplitude [8].

The numerical approximation of the dispersive shallow water equations can be useful for studying several physical problems and also in many engineering applications, where moderately long waves occur. Although the dispersive shallow water equations constitute an approximation of a higher order with respect to the nonlinear long-wave model, their numerical discretization demands for due care. In fact, owing to the different mathematical nature of the equations and the peculiar physical range in which they are used, one cannot rely upon the mere transposition of schemes which have been demonstrated to be successful for the shallow water equations (see, for instance, [9, 10]). Roughly speaking, dispersion is expected to require that a great spatial accuracy and inertia term typically play a relevant role which calls for an appropriate account of the direction of propagation of the physical disturbance.

While the approximation of the dispersive shallow water equations by finite differences is currently used by several researchers [11], the approximation by finite elements is still for the most part unexplored. Among the few examples, we can mention that some authors have adopted a sort of predictor–corrector scheme [12, 13], borrowed from the finite difference framework. The use of a Crank–Nicolson scheme for the temporal discretizations has been exploited by Goring *et al.* [14]. Katopodes and Wu have obtained excellent results adopting a Lax–Wendroff time discretization of the whole system of equations [15]. To the authors' knowledge, there is no example of 2D simulation of nonlinear dispersive waves on unstructured grids.

The aim of the present paper is to investigate the application of the Taylor–Galerkin (TG) method to the dispersive shallow water equations. The Taylor–Galerkin method was proposed by Donea to solve transient convection problems [16]. The attractive numerical properties of this method have been investigated in a few studies [17–19] which demonstrate the high phase-speed accuracy of the method as well as its selective dissipation at high spatial frequencies, ensuring almost oscillation-free solutions.

These properties, which are well known in the discretization of conservation laws with smooth solutions, suggest the adoption of the Taylor–Galerkin method for simulating the propagation of dispersive waves, where accuracy in space and time is a very crucial issue. In this paper a new scheme of Taylor–Galerkin type suitable for dispersive wave is proposed. The presence of a dispersive operator in the equations governing this kind of flow implies a twofold modification with respect to the classical Taylor–Galerkin scheme: (i) new unknowns (the time derivative of the original unknowns) have to be introduced and (ii) a parameter has to be introduced in the construction of the scheme, which provides a kind of supplementary degree of freedom allowing the scheme to attain unconditional stability.

A remarkable property of the present approach is that accurate results can be obtained by using a very simple basis of linear finite elements. The possibility of using the compact computational molecule characteristic of the Galerkin method with linear elements is

obtained at the price of doubling the number of unknowns, but is particularly attractive in 2D computations over geometrical regions of arbitrary shape and complexity.

The content of the paper is organized as follows. In Section 2 we introduce the nonlinear system of dispersive shallow water equations both in two dimensions and in one dimension. The temporal and spatial discretizations of the one-dimensional equations according to the Taylor–Galerkin methodology are described in Section 3. The resulting TG scheme was already anticipated in [20] in the context of the dispersive shallow water system. The analysis of the numerical stability of the TG scheme applied to a suitable linearized model of the equation system is presented in Section 4. In Section 5 the method is extended to two-dimensional equations, providing also a detailed discussion of the treatment of the boundary conditions. In Section 6, three computational examples in one dimension are considered, while Section 7 contains the results of a 2D simulation of a solitary wave overpassing a circular cylinder, using an unstructured triangular mesh with linear interpolation of all the unknowns. The final section is devoted to some concluding remarks.

2. THE DISPERSIVE SHALLOW WATER EQUATIONS

The dispersive shallow water equations for free surface flow read [4]

$$\frac{\partial h}{\partial t} + \boldsymbol{\nabla} \cdot (h\mathbf{v}) = 0, \tag{2.1}$$

$$\frac{\partial \mathbf{v}}{\partial t} - \frac{H}{2}\frac{\partial}{\partial t}\boldsymbol{\nabla}(\boldsymbol{\nabla} \cdot (H\mathbf{v})) + \frac{H^2}{6}\frac{\partial}{\partial t}\boldsymbol{\nabla}(\boldsymbol{\nabla} \cdot \mathbf{v}) + (\mathbf{v} \cdot \boldsymbol{\nabla})\mathbf{v} + g\boldsymbol{\nabla}\xi = 0. \tag{2.2}$$

Here $\mathbf{v}(x, y, t)$ is the vertically averaged fluid velocity, $-H(x, y)$ is the depth under a reference plane, $\xi(x, y, t)$ is the elevation over the same reference plane, $h(x, y, t) = \xi(x, y, t) + H(x, y)$, and g is the gravity field. By using the long-wave zero order approximation

$$\frac{\partial \xi}{\partial t} = -\boldsymbol{\nabla} \cdot (H\mathbf{v}), \quad \frac{\partial \mathbf{v}}{\partial t} = -g\boldsymbol{\nabla}\xi, \tag{2.3}$$

the dispersive shallow water equations can be rewritten in several forms that differ for the higher order differential terms appearing in (2.2) [7]. However, the form shown in (2.1)–(2.2) is the most convenient from the numerical point of view, as discussed in [21], and we refer to it in the present work.

When considering a one-dimensional case, the system of differential equations (2.1)–(2.2) can be formally rewritten as

$$\frac{\partial}{\partial t}\begin{pmatrix} h \\ v - \frac{H}{2}\frac{\partial^2 (Hv)}{\partial x^2} + \frac{H^2}{6}\frac{\partial^2 v}{\partial x^2} \end{pmatrix} + \begin{pmatrix} v & h \\ g & v \end{pmatrix}\frac{\partial}{\partial x}\begin{pmatrix} h \\ v \end{pmatrix} = \begin{pmatrix} 0 \\ g\frac{dH}{dx} \end{pmatrix}. \tag{2.4}$$

This system can be recast in a compact vector notation either in the conservation-law form

$$\frac{\partial}{\partial t}(1 - L)\mathbf{u} + \frac{\partial \mathbf{f}(\mathbf{u})}{\partial x} = \mathbf{s}, \tag{2.5}$$

or in the quasilinear form

$$\frac{\partial}{\partial t}(1 - L)\mathbf{u} + A(\mathbf{u})\frac{\partial \mathbf{u}}{\partial x} = \mathbf{s}, \tag{2.6}$$

where

$$\mathbf{u} = (h, v)^T, \quad \mathbf{f}(\mathbf{u}) = \left(hv, \frac{v^2}{2} + gh \right)^T, \quad A(\mathbf{u}) = \begin{pmatrix} v & h \\ g & v \end{pmatrix},$$
$$L\mathbf{u} = \left(0, \frac{H}{2} \frac{\partial^2 (Hv)}{\partial x^2} - \frac{H^2}{6} \frac{\partial^2 v}{\partial x^2} \right)^T, \quad \mathbf{s}(x) = \left(0, g \frac{dH}{dx} \right)^T. \tag{2.7}$$

Notice that L is a spatial linear operator so that it commutes with $\partial/\partial t$.

If the bottom is flat, i.e., if $H = H =$ constant, the source term cancels and the operator L simplifies to

$$L\mathbf{u} = \left(0, \frac{H^2}{3} \frac{\partial^2 v}{\partial x^2} \right)^T. \tag{2.8}$$

3. NUMERICAL SCHEME

The numerical integration of the dispersive shallow water equations requires an appropriate, i.e., directionally biased, treatment of the propagation–advection term and, at the same time, an accurate representation of the dispersive term in the equations. To cope with these two needs, the Taylor–Galerkin method [16], developed originally for the accurate solution of transient advection problems, lends itself as the most promising candidate. In fact, the fundamental aspect of the Taylor–Galerkin method is the proper matching of the time and space discretization processes for advection equations or hyperbolic systems: the discretization in time is performed before the spatial approximation by means of a Taylor series expansion in the time step, as in the classical Lax–Wendroff FD scheme [22], but the series is extended to a higher order than the second to exploit the superior approximation properties of a spatial discretization by linear finite elements [17]. In this way, a method is obtained which embodies elements of the theory of characteristics (in 1D as well as in 2D or 3D) while still retaining the compact computational molecule typical of any Galerkin finite element approximation. Notice that the issue here is not that of simply introducing a time discretization of a higher order, but that of obtaining a time discrete version of the PDE which embodies its high-order differential information at the (semi)continuous level, very similarly to the classical Obrechkoff methods for solving ODE problems.

3.1. *Temporal Discretization*

Let us perform an expansion of the quantity $\mathbf{u}^{n+1}$ in a Taylor series of Δt around time $t = t^n$; up to the third order we get

$$\mathbf{u}^{n+1} = \mathbf{u}^n + \Delta t \mathbf{u}_t^n + \frac{(\Delta t)^2}{2} \mathbf{u}_{tt}^n + \frac{(\Delta t)^3}{6} \mathbf{u}_{ttt}^n + O((\Delta t)^4), \tag{3.1}$$

where $\mathbf{u}_t^n$ is the time derivative of $\mathbf{u}$ evaluated at $t = t^n$ and so on. The third order derivative can be expressed also as

$$\mathbf{u}_{ttt}^n = \frac{\theta}{\Delta t} \left(\mathbf{u}_{tt}^{n+1} - \mathbf{u}_{tt}^n \right) + O(\epsilon_\theta), \tag{3.2}$$

where

$$\epsilon_\theta = \begin{cases} \Delta t & \text{for } \theta = 1, \\ 1 & \text{for } \theta \neq 1. \end{cases} \tag{3.3}$$

By substituting the expression (3.2) into the last term of the right-hand side of equation (3.1), we get

$$\mathbf{u}^{n+1} - \theta \frac{(\Delta t)^2}{6} \mathbf{u}_{tt}^{n+1} = \mathbf{u}^n + \Delta t \mathbf{u}_t^n + (3-\theta) \frac{(\Delta t)^2}{6} \mathbf{u}_{tt}^n + O\big((\Delta t)^3 \epsilon_\theta\big). \tag{3.4}$$

For $\theta = 1$, the expression (3.4) is third order accurate as (3.1) and coincides with the classical form used as starting step for the derivation of the Taylor–Galerkin scheme [16]. For other values of θ, the expression (3.4) is only second order accurate.

Applying the linear operator $(1 - L)$ to Eq. (3.4), we get

$$(1-L)\mathbf{u}^{n+1} - \theta \frac{(\Delta t)^2}{6} (1-L)\mathbf{u}_{tt}^{n+1} = (1-L)\mathbf{u}^n + \Delta t (1-L)\mathbf{u}_t^n + (3-\theta) \frac{(\Delta t)^2}{6} (1-L)\mathbf{u}_{tt}^n. \tag{3.5}$$

We now follow the Lax–Wendroff idea, originally pursued in a first-order hyperbolic context, and substitute the exact equation (2.5) and its time derivative in the Taylor series. Equation (2.5) reads

$$\frac{\partial}{\partial t}(1-L)\mathbf{u} = (1-L)\frac{\partial \mathbf{u}}{\partial t} = -\frac{\partial \mathbf{f}(\mathbf{u})}{\partial x} + \mathbf{s}, \tag{3.6}$$

so that

$$\frac{\partial^2}{\partial t^2}(1-L)\mathbf{u} = \frac{\partial}{\partial t}\left((1-L)\frac{\partial \mathbf{u}}{\partial t}\right) = \frac{\partial}{\partial t}\left(-\frac{\partial \mathbf{f}(\mathbf{u})}{\partial x} + \mathbf{s}(x)\right) = -\frac{\partial}{\partial t}\frac{\partial \mathbf{f}(\mathbf{u})}{\partial x}. \tag{3.7}$$

It is now possible to substitute the forms (3.6) and (3.7) into Eq. (3.5), thus getting

$$\begin{aligned}(1-L)\mathbf{u}^{n+1} + \theta \frac{(\Delta t)^2}{6} \frac{\partial}{\partial t} \frac{\partial \mathbf{f}(\mathbf{u}^{n+1})}{\partial x} &= (1-L)\mathbf{u}^n - \Delta t \frac{\partial \mathbf{f}(\mathbf{u}^n)}{\partial x} \\ &\quad - (3-\theta) \frac{(\Delta t)^2}{6} \frac{\partial}{\partial t} \frac{\partial \mathbf{f}(\mathbf{u}^n)}{\partial x} + \Delta t \mathbf{s}. \end{aligned} \tag{3.8}$$

Writing the derivative of the flux $\mathbf{f}$ in quasilinear form, it is possible to rewrite Eq. (3.8) as

$$\begin{aligned}(1-L)\mathbf{u}^{n+1} + \theta \frac{(\Delta t)^2}{6} \frac{\partial}{\partial x}\left(A^{n+1} \frac{\partial \mathbf{u}^{n+1}}{\partial t}\right) &= (1-L)\mathbf{u}^n - \Delta t \frac{\partial \mathbf{f}(\mathbf{u}^n)}{\partial x} \\ &\quad - (3-\theta) \frac{(\Delta t)^2}{6} \frac{\partial}{\partial x}\left(A^n \frac{\partial \mathbf{u}^n}{\partial t}\right) + \Delta t \mathbf{s}, \end{aligned} \tag{3.9}$$

where $A^n = A(\mathbf{u}^n)$, etc. At this stage, a difficulty, which is typical of these dispersive equations, is encountered: because of the presence of the operator L, the terms with the temporal derivatives appearing in (3.9) cannot be expressed in a straightforward manner in terms of purely spatial derivatives. To make the temporal derivatives disappear in Eq. (3.9), it is then necessary to introduce the new auxiliary variable $\mathbf{w}$, defined as

$$\mathbf{w} \equiv \frac{\partial \mathbf{u}}{\partial t} = (1-L)^{-1}\left(-\frac{\partial \mathbf{f}(\mathbf{u})}{\partial x} + \mathbf{s}\right). \tag{3.10}$$

Consequently, Eq. (3.9) is equivalent to the system of equations

$$(1-L)\mathbf{w}^{n+1} + \frac{d\mathbf{f}(\mathbf{u}^{n+1})}{dx} = \mathbf{s}, \tag{3.11}$$

$$(1-L)\mathbf{u}^{n+1} + \theta\frac{(\Delta t)^2}{6}\frac{d}{dx}(A^{n+1}\mathbf{w}^{n+1}) = (1-L)\mathbf{u}^n - \Delta t\frac{d\mathbf{f}(\mathbf{u}^n)}{dx} - (3-\theta)\frac{(\Delta t)^2}{6}\frac{d}{dx}(A^n\mathbf{w}^n) + \Delta t\mathbf{s}, \tag{3.12}$$

in which the spatial derivative has been indicated as an ordinary derivative since the equations represent a time-discretized version of the original partial differential problem. The discretization is second order accurate (third order only for $\theta = 1$) without requiring the use of an intermediate step (two-level scheme). The two (vector) equations of the system are nonlinear and are coupled together.

3.2. *Spatial Discretization*

We now consider the weak form of Eqs. (3.11)–(3.12) provided by the standard Galerkin finite element [23]. The computational domain $[x_1, x_2]$ is partitioned in equispaced intervals and we define the set of the linear functions $\{\psi_i\}$ to be the finite element basis with value 1 in the ith node and zero out of the surrounding elements. Then the weak form of Eqs. (3.11)–(3.12) reads

$$\left\langle \psi_i, (1-L)\mathbf{w}^{n+1}\right\rangle + \left\langle \psi_i, \frac{d\mathbf{f}(\mathbf{u}^{n+1})}{dx}\right\rangle = \langle \psi_i, \mathbf{s}\rangle, \tag{3.13}$$

$$\left\langle \psi_i, (1-L)\mathbf{u}^{n+1}\right\rangle - \theta\psi_i', \frac{(\Delta t)^2}{6}\langle A^{n+1}\mathbf{w}^{n+1}\rangle = \left\langle \psi_i, (1-L)\mathbf{u}^n\right\rangle - \Delta t\left\langle \psi_i, \frac{d\mathbf{f}(\mathbf{u}^n)}{dx}\right\rangle + (3-\theta)\frac{(\Delta t)^2}{6}\left\langle \psi_i', A^n\mathbf{w}^n\right\rangle + \Delta t\langle \psi_i, \mathbf{s}\rangle, \tag{3.14}$$

where $\langle\cdot,\cdot\rangle$ indicates the usual L^2 product. Some terms in Eqs. (3.13)–(3.14) have been integrated by parts; this operation yields to boundary integrals, which vanish in the present context because of the boundary conditions (see the discussion about this issue at the end of Section 5).

To solve Eqs. (3.13)–(3.14) numerically, they have to be linearized. We can adopt, for instance, the most simple linearization

$$A^{n+1}\mathbf{w}^{n+1} \simeq A^n\mathbf{w}^{n+1} \tag{3.15}$$

and similarly in the implicit term involving the flux

$$\frac{d\mathbf{f}(\mathbf{u}^{n+1})}{dx} \simeq A^n\mathbf{u}_x^{n+1}. \tag{3.16}$$

The resulting linearized system is

$$\left\langle \psi_i, (1-L)\mathbf{w}^{n+1}\right\rangle + \left\langle \psi_i, A^n\frac{d\mathbf{u}^{n+1}}{dx}\right\rangle = \langle \psi_i, \mathbf{s}\rangle, \tag{3.17}$$

$$\langle \psi_i, (1-L)\mathbf{u}^{n+1}\rangle - \theta\frac{(\Delta t)^2}{6}\langle \psi_i', A^n\mathbf{w}^{n+1}\rangle = \langle \psi_i, (1-L)\mathbf{u}^n\rangle - \Delta t\left\langle \psi_i, \frac{d\mathbf{f}(\mathbf{u}^n)}{dx}\right\rangle + (3-\theta)\frac{(\Delta t)^2}{6}\langle \psi_i', A^n\mathbf{w}^n\rangle + \Delta t\langle \psi_i, \mathbf{s}\rangle. \tag{3.18}$$

Projecting the solution $\mathbf{u}^{n+1}$ on the space of the ψ_i, we get

$$\mathbf{u}^{n+1}(x) = \sum_j \psi_j(x)\mathbf{u}_j^{n+1}, \quad \mathbf{w}^{n+1}(x) = \sum_j \psi_j(x)\mathbf{w}_j^{n+1}, \tag{3.19}$$

and, as $A(\mathbf{u})$ depends linearly on $\mathbf{u}$, we can define

$$\mathbf{u}_j^{n+1} = \left(h_j^{n+1}, v_j^{n+1}\right), \quad A_j^{n+1} = \begin{pmatrix} v_j^{n+1} & h_j^{n+1} \\ g & v_j^{n+1}\end{pmatrix}. \tag{3.20}$$

Equations (3.17)–(3.18) can then be rewritten as

$$\sum_j \langle \psi_i, (1-L)\psi_j\rangle \mathbf{w}_j^{n+1} + \sum_{k,j}\langle \psi_i, \psi_k\psi_j'\rangle A_k^n\mathbf{u}_j^{n+1} = \langle \psi_i, \mathbf{s}\rangle, \tag{3.21}$$

$$\begin{aligned}\sum_j \langle \psi_i, (1-L)\psi_j\rangle \mathbf{u}_j^{n+1} - \theta\frac{(\Delta t)^2}{6}\sum_{k,j}\langle \psi_i', \psi_k\psi_j\rangle A_k^n\mathbf{w}_j^{n+1} \\ = \sum_j \langle \psi_i, (1-L)\psi_j\rangle \mathbf{u}_j^n - \Delta t\sum_{k,j}\langle \psi_i, \psi_k\psi_j'\rangle A_k^n\mathbf{u}_j^n \\ + (3-\theta)\frac{(\Delta t)^2}{6}\sum_{k,j}\langle \psi_i', \psi_k\psi_j\rangle A_k^n\mathbf{w}_j^n + \Delta t\langle \psi_i, \mathbf{s}\rangle.\end{aligned} \tag{3.22}$$

These equations constitute a linear system in the unknowns $(\mathbf{w}_j^{n+1}, \mathbf{u}_j^{n+1})$, the dependence of A_j^n on $\mathbf{u}_j^n$ being explicitly given in (3.20).

The terms involving the operator L are evaluated using the usual integration by parts:

$$\begin{aligned}\langle \psi_i, (1-L)\psi_j\rangle &= \langle \psi_i, \psi_j\rangle - \langle L\psi_i, \psi_j\rangle \\ &= \langle \psi_i, \psi_j\rangle + \frac{1}{2}\left\langle \frac{d}{dx}(H\psi_i), \frac{d}{dx}(H\psi_j)\right\rangle - \frac{1}{6}\left\langle \frac{d}{dx}(H^2\psi_i), \frac{d\psi_j}{dx}\right\rangle \\ &\quad + \text{boundary terms.}\end{aligned} \tag{3.23}$$

It may be noticed that the operator L is symmetric only for $H = H =$ constant.

Remarks on the discrete equation system. Equations (3.21)–(3.22) constitute a linear system to be solved for determining the solution $\mathbf{u}^{n+1}$. The linear system comprises the vector unknowns $(\mathbf{w}_j^{n+1}, \mathbf{u}_j^{n+1})$, each with two scalar components. If N is the number of nodes, the order of the linear system is therefore $4N$. In general, the matrix is nonsymmetric and block-tridiagonal, with 4×4 blocks.

It is interesting to consider the simpler form assumed by the system (3.21)–(3.22) when a scheme of lower time accuracy is considered or when the "dispersion operator" L is absent.

For $\theta = 0$ or, equivalently, if the Taylor series (3.1) is limited to the second order term, the final linear system to be solved can be written as

$$\sum_j \langle \psi_i, (1-L)\psi_j \rangle \mathbf{w}_j^{n+1} = -\sum_{k,j} \langle \psi_i, \psi_k \psi_j' \rangle A_k^n \mathbf{u}_j^{n+1} + \langle \psi_i, \mathbf{s} \rangle, \tag{3.24}$$

$$\sum_j \langle \psi_i, (1-L)\psi_j \rangle \mathbf{u}_j^{n+1} = \sum_j \langle \psi_i, (1-L)\psi_j \rangle \mathbf{u}_j^n - \Delta t \sum_{k,j} \langle \psi_i, \psi_k \psi_j' \rangle A_k^n \mathbf{u}_j^n + \frac{(\Delta t)^2}{2} \sum_{k,j} \langle \psi_i', \psi_k \psi_j \rangle A_k^n \mathbf{w}_j^n + \Delta t \langle \psi_i, \mathbf{s} \rangle. \tag{3.25}$$

In fact, one can solve for $\mathbf{u}_j^{n+1}$ from the second equation before solving the first one for $\mathbf{w}_j^{n+1}$, which can be addressed in a subsequent step. Furthermore, due to the form of the operator L, each of these subsystems uncouples in two systems of N unknowns for the two scalar components of the vectors unknowns. Therefore, in this case the 4×4 block-tridiagonal system uncouples into four scalar tridiagonal systems of N equations. In the particular case of a flat bottom, the scalar tridiagonal systems are symmetric, thanks to the symmetry of operator L. This is the Lax–Wendroff type scheme proposed by Katopodes and Wu [15].

If $L = 0$ (shallow water equations), Eq. (3.10) is trivial and the expression of $\mathbf{w}$ can be directly substituted in Eq. (3.11). The order of the block-tridiagonal system is now $2N$. In particular, for $\theta = 1$ this method is nothing but the Taylor–Galerkin scheme applied to a hyperbolic system.

4. LINEAR STABILITY ANALYSIS

To analyze the numerical stability of the scheme (3.21)–(3.22), it is useful, for the sake of simplicity, to consider the regularized long wave equation [24]. This equation is the linear scalar counterpart of the dispersive shallow water system and describes the propagation of waves traveling in one direction only, on a flat bottom [8]:

$$\frac{\partial u}{\partial t} + \left(\frac{3}{2} u + \sqrt{gH} \right) \frac{\partial u}{\partial x} - \frac{H^2}{3} \frac{\partial}{\partial t} \frac{\partial^2 u}{\partial x^2} = 0. \tag{4.1}$$

To assess the stability properties of the new TG scheme, at least in the linear regime, we introduce the linearized version of Eq. (4.1), which reads

$$\frac{\partial u}{\partial t} + a \frac{\partial u}{\partial x} - b \frac{\partial}{\partial t} \frac{\partial^2 u}{\partial x^2} = 0, \tag{4.2}$$

where a and b are positive constants. Considering linear interpolation functions on a (periodic) uniform grid of N equal linear elements, the discrete equations (3.21)–(3.22) can be recast in the well-known finite difference format (see, for instance, [25]), and the Taylor–Galerkin scheme (3.18)–(3.19) applied to Eq. (4.2) assumes the form

$$\frac{1}{6}\left(w_{j-1}^{n+1} + 4w_j^{n+1} + w_{j+1}^{n+1}\right) - \frac{b}{(\Delta x)^2}\left(w_{j-1}^{n+1} - 2w_j^{n+1} + w_{j+1}^{n+1}\right) + \frac{a}{2\Delta x}\left(u_{j+1}^{n+1} - u_{j-1}^{n+1}\right) = 0, \tag{4.3}$$

$$\frac{1}{6}\left(u_{j-1}^{n+1}+4u_j^{n+1}+u_{j+1}^{n+1}\right)-\frac{b}{(\Delta x)^2}\left(u_{j-1}^{n+1}-2u_j^{n+1}+u_{j+1}^{n+1}\right)+a\theta\frac{(\Delta t)^2}{12}\left(w_{j+1}^{n+1}-w_{j-1}^{n+1}\right)$$
$$=\frac{1}{6}\left(u_{j-1}^{n}+4u_j^{n}+u_{j+1}^{n}\right)-\frac{b}{(\Delta x)^2}\left(u_{j-1}^{n}-2u_j^{n}+u_{j+1}^{n}\right)-a\frac{\Delta t}{2\Delta x}\left(u_{j+1}^{n}-u_{j-1}^{n}\right)$$
$$-(3-\theta)\frac{(\Delta t)^2}{12}\left(w_{j+1}^{n}-w_{j-1}^{n}\right). \tag{4.4}$$

We now consider the error of the scheme, defined as the difference between the exact and the computed solution. Denoting by η_j^n, ϵ_j^n the round-off error for w_j^n, u_j^n, respectively, these quantities can be expanded in a Fourier series as

$$\eta_j^n=\sum_\phi \eta_\phi^n\, e^{ij\phi},\quad \epsilon_j^n=\sum_\phi \epsilon_\phi^n\, e^{ij\phi}, \tag{4.5}$$

where $\phi=\phi_k=k\pi/N$. As the truncation error satisfies the same equation of the discrete solution, substituting the form (4.5) into Eqs. (4.3)–(4.4) and carrying out some elementary algebra, the error components are found to satisfy the system

$$\left[\frac{1}{3}(2+\cos\phi)+\frac{2b}{(\Delta x)^2}(1-\cos\phi)\right]\eta_\phi^{n+1}+i\,\frac{a}{\Delta x}\sin\phi\,\epsilon_\phi^{n+1}=0, \tag{4.6}$$

$$\left[\frac{1}{3}(2+\cos\phi)+\frac{2b}{(\Delta x)^2}(1-\cos\phi)\right]\epsilon_\phi^{n+1}+i\theta\frac{a(\Delta t)^2}{6\Delta x}\sin\phi\,\eta_\phi^{n+1}$$
$$=\left[\frac{1}{3}(2+\cos\phi)+\frac{2b}{(\Delta x)^2}(1-\cos\phi)\right]\epsilon_\phi^{n}-i\,\frac{a\Delta t}{\Delta x}\sin\phi\,\epsilon_\phi^{n}-i(3-\theta)\frac{a(\Delta t)^2}{6\Delta x}\sin\phi\,\eta_\phi^{n} \tag{4.7}$$

To simplify the analysis, it is convenient to introduce the quantities

$$\alpha=a\frac{\Delta t}{\Delta x}\sin\phi\quad\text{and}\quad\beta=\frac{1}{3}(2+\cos\phi)+\frac{2b}{(\Delta x)^2}(1-\cos\phi), \tag{4.8}$$

where it can be noted that $\beta>0$ for any ϕ. Then, Eqs. (4.6)–(4.7) may be rewritten as

$$\beta\eta_\phi^{n+1}+\frac{i\alpha}{\Delta t}\epsilon_\phi^{n+1}=0, \tag{4.9}$$

$$\beta\epsilon_\phi^{n+1}+i\theta\frac{\alpha\Delta t}{6}\eta_\phi^{n+1}=(\beta-i\alpha)\,\epsilon_\phi^{n}-i(3-\theta)\frac{\alpha\Delta t}{6}\eta_\phi^{n}. \tag{4.10}$$

Substituting the former expression into the latter, we find

$$\left(\beta+\theta\frac{\alpha^2}{6\beta}\right)\epsilon_\phi^{n+1}=\left[\beta-i\alpha-(3-\theta)\frac{\alpha^2}{6\beta}\right]\epsilon_\phi^{n}, \tag{4.11}$$

or

$$\frac{\epsilon_\phi^{n+1}}{\epsilon_\phi^{n}}=\frac{6\beta^2-i6\alpha\beta-(3-\theta)\alpha^2}{6\beta^2+\theta\alpha^2}. \tag{4.12}$$

The numerical stability of the scheme is controlled by the magnitude of the amplification factor above and it is guaranteed provided that

$$\left|\frac{\epsilon_\phi^{n+1}}{\epsilon_\phi^n}\right|^2 = \frac{[6\beta^2 - (3-\theta)\alpha^2]^2 + 36\alpha^2\beta^2}{(6\beta^2 + \theta\alpha^2)^2} \leq 1. \tag{4.13}$$

It is very simple to show that such a condition is verified, for any values of α and β, provided that

$$\theta \geq \frac{3}{2}. \tag{4.14}$$

Therefore, for θ satisfying this unequality the proposed scheme is unconditionally stable. Note that the marginal value $\theta = \frac{3}{2}$ yields to a zero dissipative scheme. On the contrary, for $\theta = \frac{1}{2}$, that is, for the standard Taylor–Galerkin coefficients of the second order terms, the scheme is always unstable. This is due to the modification of the scheme caused by the introduction of the unknown w.

Absence of numerical diffusivity is a very important feature for the discretization of nonlinear dispersive equations that typically admit as a solution waves traveling without distortion. The permanent shape of these solutions can be assured only by the exact balancing of convection and dispersion. This property has to be accurately preserved by the numerical scheme and requires avoiding introducing spurious numerical diffusion.

5. EXTENSION TO THE TWO-DIMENSIONAL SYSTEM

In this section the numerical scheme (3.18)–(3.19) derived in Section 3 is extended to the two-dimensional equations. For the sake of simplicity, we restrict our attention to the equations modeling the flow on a horizontal bottom $H = H =$ constant. In this case the dispersive shallow water equations read

$$\xi_t + \nabla \cdot (h\mathbf{v}) = 0, \tag{5.1}$$

$$\mathbf{v}_t - \frac{H^2}{3}\nabla(\nabla \cdot \mathbf{v}_t) + (\mathbf{v} \cdot \nabla)\mathbf{v} + g\nabla\xi = 0. \tag{5.2}$$

Analogously to the 1D case, the momentum equation can be rewritten in a more compact form by introducing the multidimensional spatial differential operator L,

$$L\mathbf{v} = \frac{H^2}{3}\nabla(\nabla \cdot \mathbf{v}), \tag{5.3}$$

so that Eq. (5.2) simplifies to

$$(1 - L)\mathbf{v}_t + (\mathbf{v} \cdot \nabla)\mathbf{v} + g\nabla\xi = 0. \tag{5.4}$$

It can be noted that in two dimensions the equations cannot be written in a conservative form similar to (2.5). We then introduce auxiliary unknowns which are the time derivatives of the basic unknowns, namely,

$$\zeta \equiv \xi_t = -\nabla \cdot (h\mathbf{v}), \tag{5.5}$$

$$\boldsymbol{\nu} \equiv \mathbf{v}_t = (1 - L)^{-1}[-(\mathbf{v} \cdot \nabla)\mathbf{v} - g\nabla\xi]. \tag{5.6}$$

In analogy with the 1D case, to derive the numerical scheme a Taylor expansion in Δt up to third order has to be performed for both ξ and $\mathbf{v}$:

$$\xi^{n+1} = \xi^n + \Delta t \xi_t^n + \frac{(\Delta t)^2}{2}\xi_{tt}^n + \frac{(\Delta t)^3}{6}\xi_{ttt}^n, \tag{5.7}$$

$$\mathbf{v}^{n+1} = \mathbf{v}^n + \Delta t \mathbf{v}_t^n + \frac{(\Delta t)^2}{2}\mathbf{v}_{tt}^n + \frac{(\Delta t)^3}{6}\mathbf{v}_{ttt}^n. \tag{5.8}$$

We observe that the third order derivative can be rewritten as

$$\xi_{ttt}^n = \frac{\theta}{\Delta t}\left(\xi_{tt}^{n+1} - \xi_{tt}^n\right) + O(\epsilon_\theta), \tag{5.9}$$

$$\mathbf{v}_{ttt}^n = \frac{\theta}{\Delta t}\left(\mathbf{v}_{tt}^{n+1} - \mathbf{v}_{tt}^n\right) + O(\epsilon_\theta), \tag{5.10}$$

where ϵ_θ is defined as in (3.3). Equations (5.9)–(5.10) allow us to rewrite (5.7)–(5.8) as

$$\xi^{n+1} - \theta\frac{(\Delta t)^2}{6}\xi_{tt}^{n+1} = \xi^n + \Delta t \xi_t^n + (3-\theta)\frac{(\Delta t)^2}{6}\xi_{tt}^n, \tag{5.11}$$

$$\mathbf{v}^{n+1} - \theta\frac{(\Delta t)^2}{6}\mathbf{v}_{tt}^{n+1} = \mathbf{v}^n + \Delta t \mathbf{v}_t^n + (3-\theta)\frac{(\Delta t)^2}{6}\mathbf{v}_{tt}^n. \tag{5.12}$$

The original Eqs. (5.1)–(5.4) can then be substituted into (5.11)–(5.12), yielding

$$\xi^{n+1} + \theta\frac{(\Delta t^2)}{6}\boldsymbol{\nabla}\cdot(h^{n+1}\mathbf{v}^{n+1})_t = \xi^n - \Delta t\boldsymbol{\nabla}\cdot(h^n\mathbf{v}^n) - (3-\theta)\frac{(\Delta t)^2}{6}\boldsymbol{\nabla}\cdot(h^n\mathbf{v}^n)_t, \tag{5.13}$$

$$\begin{aligned}(1-L)\mathbf{v}^{n+1} &+ \theta\frac{(\Delta t)^2}{6}[(\mathbf{v}^{n+1}\cdot\boldsymbol{\nabla})\mathbf{v}^{n+1} + g\boldsymbol{\nabla}\xi^{n+1}]_t \\ &= (1-L)\mathbf{v}^n - \Delta t[(\mathbf{v}^n\cdot\boldsymbol{\nabla})\mathbf{v}^n + g\boldsymbol{\nabla}\xi^n] - (3-\theta)\frac{(\Delta t)^2}{6}[(\mathbf{v}^n\cdot\boldsymbol{\nabla})\mathbf{v}^n + g\boldsymbol{\nabla}\xi^n]_t.\end{aligned} \tag{5.14}$$

Then, using the definitions (5.5)–(5.6), the following discretization in time is obtained:

$$\zeta^{n+1} + \boldsymbol{\nabla}\cdot(h^{n+1}\mathbf{v}^{n+1}) = 0, \tag{5.15}$$

$$(1-L)\boldsymbol{\nu}^{n+1} + (\mathbf{v}^{n+1}\cdot\boldsymbol{\nabla})\mathbf{v}^{n+1} + g\boldsymbol{\nabla}\xi^{n+1} = 0, \tag{5.16}$$

$$\begin{aligned}\xi^{n+1} &+ \theta\frac{(\Delta t)^2}{6}\boldsymbol{\nabla}\cdot(\zeta^{n+1}\mathbf{v}^{n+1} + h^{n+1}\boldsymbol{\nu}^{n+1}) \\ &= \xi^n - \Delta t\boldsymbol{\nabla}\cdot(h^n\mathbf{v}^n) - (3-\theta)\frac{(\Delta t)^2}{6}\boldsymbol{\nabla}\cdot(\zeta^n\mathbf{v}^n + h^n\boldsymbol{\nu}^n),\end{aligned} \tag{5.17}$$

$$\begin{aligned}(1-L)\mathbf{v}^{n+1} &+ \theta\frac{(\Delta t)^2}{6}[(\boldsymbol{\nu}^{n+1}\cdot\boldsymbol{\nabla})\mathbf{v}^{n+1} + (\mathbf{v}^{n+1}\cdot\boldsymbol{\nabla})\boldsymbol{\nu}^{n+1} + g\boldsymbol{\nabla}\zeta^{n+1}] \\ &= (1-L)\mathbf{v}^n - \Delta t[(\mathbf{v}^n\cdot\boldsymbol{\nabla})\mathbf{v}^n + g\boldsymbol{\nabla}\xi^n] \\ &\quad - (3-\theta)\frac{(\Delta t)^2}{6}[(\boldsymbol{\nu}^n\cdot\boldsymbol{\nabla})\mathbf{v}^n + (\mathbf{v}^n\cdot\boldsymbol{\nabla})\boldsymbol{\nu}^n + g\boldsymbol{\nabla}\zeta^n].\end{aligned} \tag{5.18}$$

We linearize the equations above as

$$\zeta^{n+1} + h^n\boldsymbol{\nabla}\cdot\mathbf{v}^{n+1} + \mathbf{v}^n\cdot\boldsymbol{\nabla}h^{n+1} = 0, \tag{5.19}$$

$$(1-L)\boldsymbol{\nu}^{n+1} + (\mathbf{v}^n\cdot\boldsymbol{\nabla})\mathbf{v}^{n+1} + g\boldsymbol{\nabla}\xi^{n+1} = 0, \tag{5.20}$$

$$\xi^{n+1} + \theta\frac{(\Delta t)^2}{6}(\zeta^n \nabla\cdot\mathbf{v}^{n+1} + \mathbf{v}^n\cdot\nabla\zeta^{n+1} + h^n\nabla\cdot\boldsymbol{\nu}^{n+1} + \boldsymbol{\nu}^n\cdot\nabla h^{n+1})$$
$$= \xi^n - \Delta t\nabla\cdot(h^n\mathbf{v}^n) - (3-\theta)\frac{(\Delta t)^2}{6}\nabla\cdot(\zeta^n\mathbf{v}^n + h^n\boldsymbol{\nu}^n), \tag{5.21}$$

$$(1-L)\mathbf{v}^{n+1} + \theta\frac{(\Delta t)^2}{6}[(\boldsymbol{\nu}^n\cdot\nabla)\mathbf{v}^{n+1} + (\mathbf{v}^n\cdot\nabla)\boldsymbol{\nu}^{n+1} + g\nabla\zeta^{n+1}]$$
$$= (1-L)\mathbf{v}^n - \Delta t[(\mathbf{v}^n\cdot\nabla)\mathbf{v}^n + g\nabla\xi^n] - (3-\theta)\frac{(\Delta t)^2}{6}[(\boldsymbol{\nu}^n\cdot\nabla)\mathbf{v}^n$$
$$+ (\mathbf{v}^n\cdot\nabla)\boldsymbol{\nu}^n + g\nabla\zeta^n]. \tag{5.22}$$

The weak form of the equations is then obtained by means of the standard Galerkin method, integrating by parts, as usual, all the second order spatial derivatives. The finite element discretization of Eqs. (5.19)–(5.22) is finally accomplished using linear triangular finite elements. The procedure is fully analogous to the 1D case (except for the boundary conditions that are discussed below) and is not repeated here. The linear system to be solved in the fully discrete case involves $6N$ unknowns, N being the number of nodes of the computational mesh.

Boundary conditions. At inflow and outflow, the number of boundary conditions to be prescribed for $(\mathbf{v}, \xi)$ is dictated by the characteristic theory. We have adopted

$$\mathbf{v}\cdot\mathbf{t} = 0, \quad \xi = 0 \quad \text{at inflow}, \tag{5.23}$$
$$\xi = 0 \quad \text{at outflow}, \tag{5.24}$$

where $\mathbf{t}$ is the unit vector tangential to the boundary. At the wall, the free slip boundary condition has to be prescribed for an inviscid fluid,

$$\mathbf{v}\cdot\mathbf{n} = 0 \quad \text{at the wall}, \tag{5.25}$$

where $\mathbf{n}$ is the unit vector normal to the boundary. Moreover, boundary conditions on the auxiliary unknowns have to be prescribed. Applying the Green formula to the third order mixed derivative term of Eq. (5.2) one gets

$$\langle\Phi, \nabla(\nabla\cdot\mathbf{v}_t)\rangle = -\langle\nabla\cdot\Phi, \nabla\cdot\mathbf{v}_t\rangle + \int_\Gamma(\Phi\cdot\mathbf{n})(\nabla\cdot\mathbf{v}_t)\,d\Gamma. \tag{5.26}$$

Therefore, the natural boundary conditions to be applied for the auxiliary unknown $\boldsymbol{\nu}\equiv\mathbf{v}$ (on the portion of the boundary where the normal component of $\mathbf{v}$ is not prescribed) is

$$\nabla\cdot\mathbf{v}_t = 0, \quad \text{on all the boundary}. \tag{5.27}$$

6. NUMERICAL EXAMPLES IN ONE DIMENSION

For discussing and comparing the numerical results, in this section it turns out to be useful to rewrite the equations in terms of dimensionless variables, defined by

$$\bar{\mathbf{u}} = \frac{\mathbf{u}}{\sqrt{gH}}, \quad \bar{h} = \frac{h}{H}, \quad \bar{x} = \frac{x}{H}, \quad \bar{t} = \left(\frac{g}{H}\right)^{1/2} t. \tag{6.1}$$

Using only dimensionless variables from now on, the bar can be omitted and Eqs. (5.1)–(5.2) in dimensionless form read

$$\xi_t + \nabla \cdot (h\mathbf{v}) = 0, \tag{6.2}$$

$$\mathbf{v}_t - \tfrac{1}{3}\nabla(\nabla \cdot \mathbf{v}_t) + (\mathbf{v} \cdot \nabla)\mathbf{v} + \nabla\xi = 0. \tag{6.3}$$

6.1. *Traveling Solitary Wave*

Nonlinear dispersive systems are characterized by the fact that they admit solutions which are waves traveling without distortion, the effect of nonlinearity being balanced exactly by that of dispersion. Exact solutions of this kind exist for the dispersive shallow water equations (6.2)–(6.3), too.

For small elevation of the water with respect to the depth, it may be seen that, neglecting higher order terms, the well-known solitary wave with a sech-profile (due to Boussinesq himself) is a solution of the system (6.2)–(6.3); see [8]. The sech-profile has been used by a number of authors as an approximate initial condition for the numerical approximation of the dispersive shallow water equations [4, 12, 13, 26, 27]. However, when testing a numerical scheme, it is preferable to deal with exact solutions of the differential problem, to be able to determine the exact numerical error. For this purpose, the knowledge of *exact* solutions of the dispersive shallow water equations which have a permanent shape is necessary. This issue has been addressed in [28], where it is shown that the search for a permanent shape wave solution of the dispersive shallow water equations (6.2)–(6.3) leads, for any height of the wave, to solve an ordinary differential equation. A closed form for the propagation speed of a solitary wave is given, allowing an exact evaluation of possible numerical phase shifts induced by a numerical scheme. The derivation of a solution of this kind obtained in [28] is sketched in the Appendix for completeness of the exposition. The numerical solution of the ODE (A.1) is used in this section as the initial condition to check how accurately the TG method computes the propagation of a solitary wave. The computational mesh is intentionally rather coarse to illustrate better the performance of the scheme.

We first consider the case of a maximum elevation $\xi_0 = 0.2$ which corresponds to $\zeta_0 = 0.2$ of the Appendix. The wave is initially centered in $x = 20$ and travels up to $t = 60$. The mesh size is 0.5 and the temporal increment is 0.3.

Figure 1 shows the water elevation computed by the scheme (3.18)-(3.19) with $\theta = \frac{3}{2}$ at various instants of time. The results can be compared with those obtained by a standard Crank–Nicolson scheme (Fig. 2). The Taylor–Galerkin scheme is found be very accurate, neither showing variations in the maximum elevation of the wave nor producing an erroneous wake. The solution travels with the correct celerity (A.2) and does not suffer from the phase-lag error characteristic of other numerical schemes [29].

Figure 3 shows the computed solution in a test analogous to the previous one, but with $\xi_0 = 0.7$ This elevation falls outside of the range of applicability of the dispersive shallow water equations, since it contradicts the assumptions under which they have been derived. However, such a computation is useful to verify the robustness of the new numerical scheme. For this computation a time step $\Delta t = 0.157$ has been used. By using a finer and finer mesh, a perfect superposition of the computed and the exact solution is achieved.

6.2. *Solitary Wave on a Beach*

Here we address the simulation of a wave moving on a sloping beach, under the same conditions proposed by Peregrine [4]. The slope of the beach is $\frac{1}{30}$; the initial conditions

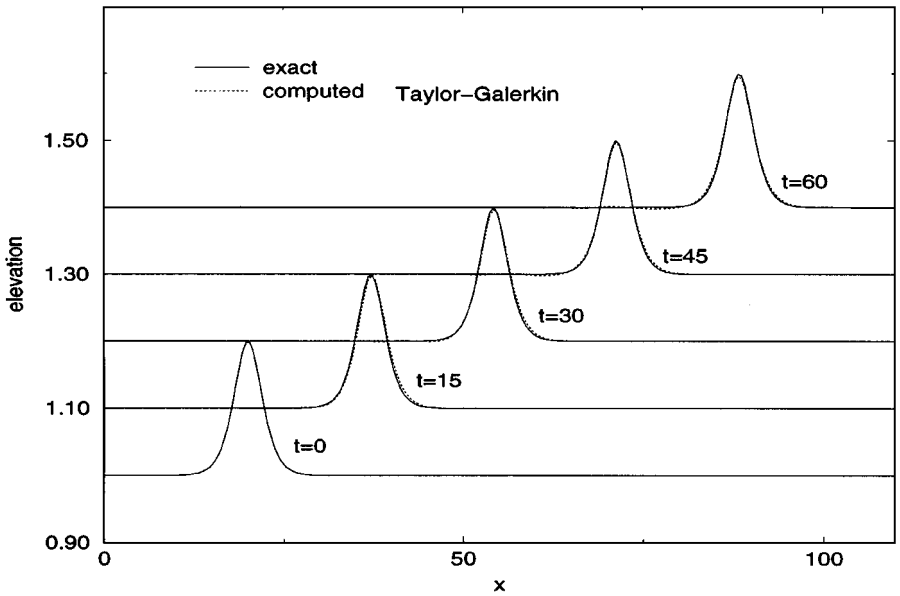

FIG. 1. Solitary wave propagation, $\xi_0 = 0.2$, Taylor–Galerkin scheme.

correspond to the ones of a solitary wave on flat bottom, centered at $x = 30$. The initial elevation of the wave is 0.1 and 0.2.

A time step $\Delta t = 0.21$ has been used and a spatial mesh size $\Delta x = 0.33$ has been assumed. Figures 4 and 5 show the elevation profile at equally spaced intervals of time. The last sketch of Fig. 4 refers to $t = 25.84$; the last sketch of Fig. 5 refers to $t = 18.6$ of elapsed time. The computation is run nearly until the ratio of elevation over depth does not overcome the assumptions of the dispersive shallow water theory.

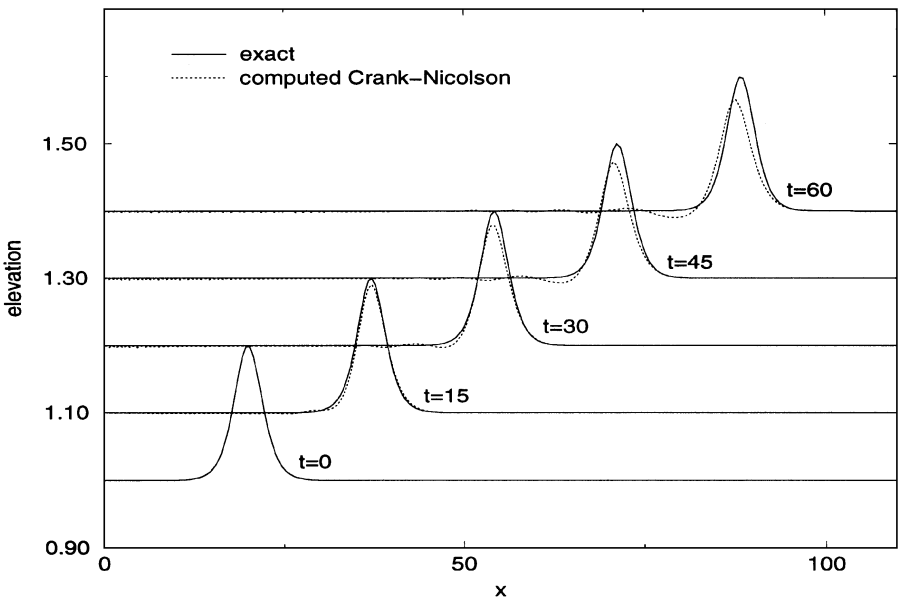

FIG. 2. Solitary wave propagation, $\xi_0 = 0.2$, Crank–Nicolson scheme.

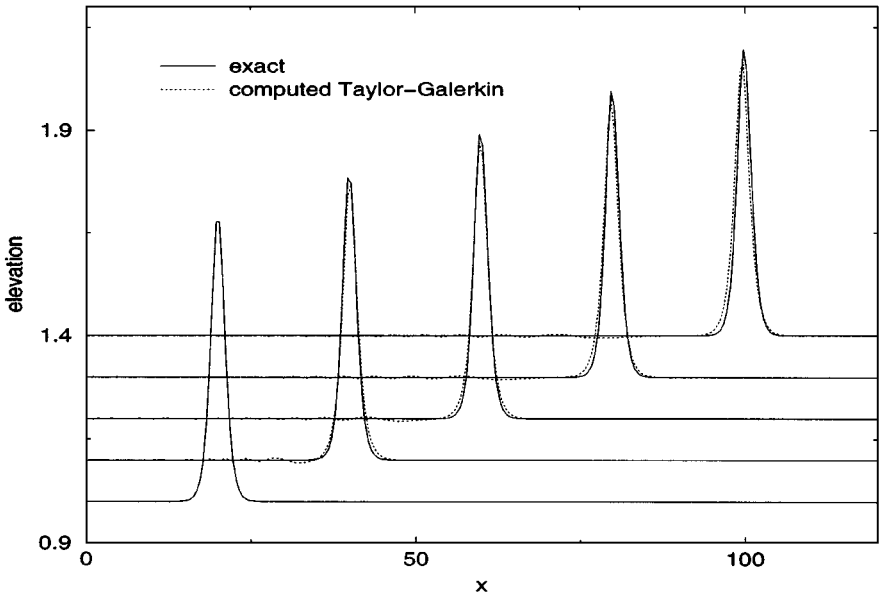

FIG. 3. Solitary wave propagation, $\xi_0 = 0.7$, Taylor–Galerkin scheme.

6.3. *Head-on Collision of Solitary Waves*

The nonlinear dispersive shallow water equations (6.2)–(6.3) allow propagation of 1D waves in both directions of the x axis. It is then interesting to simulate numerically the collision of two solitary waves traveling in opposite directions to check if the shape of the waves is preserved after collision. In other words, one can check numerically if the solitary waves solution of Eqs. (6.2)–(6.3) are solitons. We consider here two solitary waves of equal amplitude 0.5, traveling in opposite directions. This problem is equivalent to considering the reflection of a solitary wave from a wall and has been addressed, for instance, in [26, 30] (the latter for a slightly different set of equations).

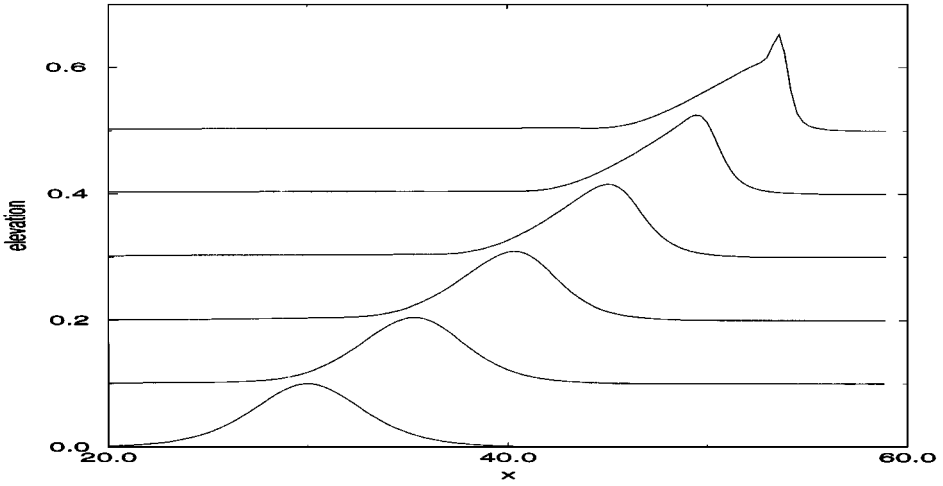

FIG. 4. Solitary wave on a beach, $\xi_0 = 0.1$.

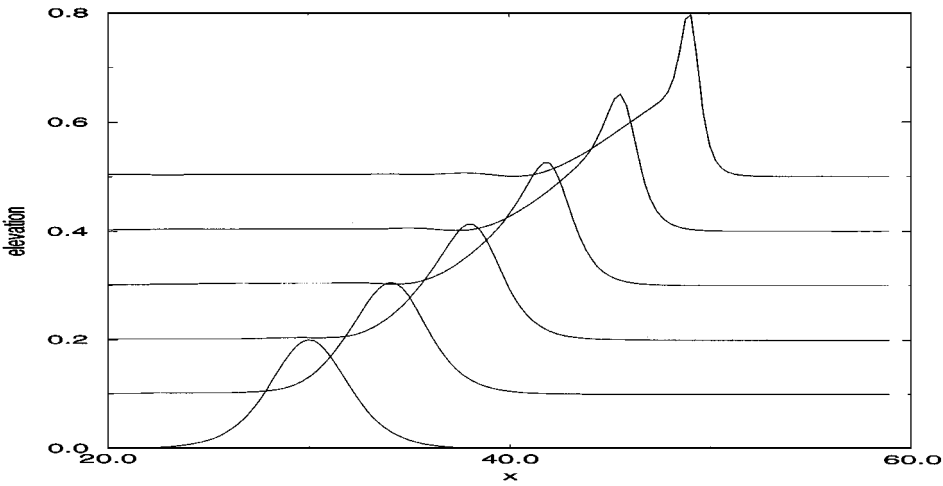

FIG. 5. Solitary wave on a beach, $\xi_0 = 0.2$.

A spatial increment $\Delta x = 0.1$ has been used with $\Delta t = 0.05$. Figure 6 shows the elevation of the water at different times before and after the collision, with a time difference of 2.5. The maximum value reached by water level is 1.0784, which is more than twice the incident wave height and is slightly different from the value 1.0504 found in [26]. After the collision, the waves continue to travel with a shape almost unchanged, but not exactly the same, as may be seen in Fig. 7. In this plot a magnification of the vertical axis makes it visible small spatial oscillations of the last profile represented in Fig. 6. This drawing shows a very small tail, with maximum amplitude which is about $1/500$ of the amplitude of the incident wave. Such results are very close to the ones obtained in [26] by a completely different numerical approach, then confirming that the solitary wave solutions of Eqs. (6.2)–(6.3) are not solitons.

Conservativity of the scheme. The integrals of some scalar quantities are conserved by Eqs. (6.2)–(6.3). In the following table the global mass and velocity at initial and final times are compared for the computations performed in the preceding paragraphs. The traveling wave values refer to the case $\xi_0 = 0.2$.

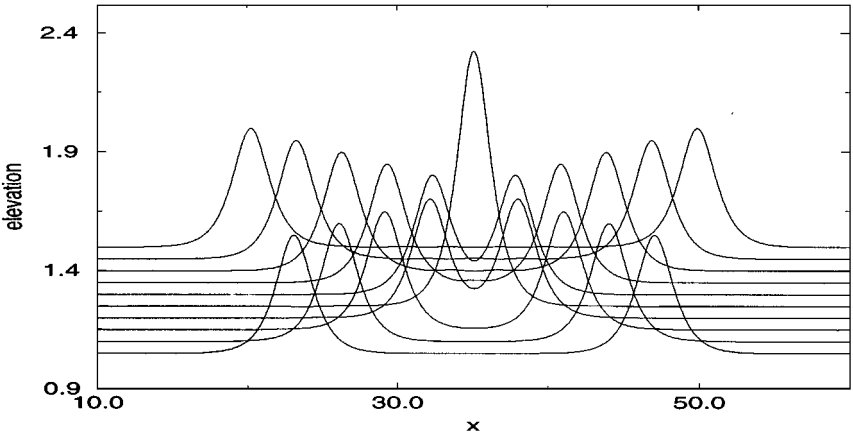

FIG. 6. Collision between two solitary waves of equal amplitude 0.5.

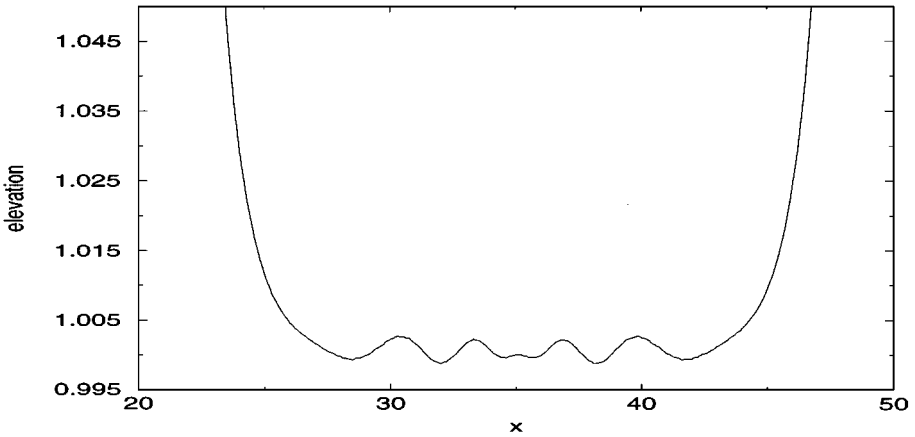

FIG. 7. Tail between the solitary waves after their head-on interaction.

Test	Δt	Δx	Initial mass	Final mass	% error
Traveling wave	0.15	0.5	1.04466	1.04640	1.6×10^{-3}
Traveling wave	0.3	0.5	1.04466	1.04381	8.1×10^{-4}
Traveling wave	0.15	0.25	1.04466	1.04437	2.7×10^{-4}
Traveling wave	0.3	0.25	1.04466	1.04477	1.1×10^{-4}
Colliding waves	0.05	0.1	3.34177	3.34229	1.5×10^{-4}
Test	Δt	Δx	Initial velocity	Final velocity	% error
Traveling wave	0.15	0.5	1.01193	1.00712	4.7×10^{-3}
Traveling wave	0.3	0.5	1.01193	1.01057	1.3×10^{-3}
Traveling wave	0.15	0.25	1.01193	1.00999	1.9×10^{-3}
Traveling wave	0.3	0.25	1.01193	1.01131	6.1×10^{-4}
Colliding waves	0.05	0.1	0	-0.00004	4.0×10^{-5}

7. SOLITARY WAVE OVER PASSING A VERTICAL CYLINDER

As an example of the performance of the scheme in two dimensions, the numerical simulation of the scattering of a solitary wave by a vertical circular cylinder has been addressed. The same problem has been already discussed in [12, 31]. Here the same geometrical data and initial conditions used in [31] have been chosen.

To study the diffraction and scattering of solitary waves by obstacles, it is convenient to introduce two dynamic dimensionless parameters

$$K_w = \frac{H\xi_0}{D^2} \quad \text{and} \quad K_D = \frac{D^2\xi_0}{H^3}, \tag{7.1}$$

where ξ_0 is the (dimensional) amplitude of the incident solitary wave traveling on water of uniform depth H and D is the horizontal width of the obstacle. The first parameter is a generalization of the Keulegan–Carpenter number to the case of solitary waves and gives information about the importance of viscous effects [31]. For $K_w \ll 1$ no separation occurs and an inviscid model is adequate. The second parameter is a measure of the relevance

of wave diffraction by the obstacle. It may be expected that diffraction and scattering are significant for $K_D \geq 1$.

Here we consider flow conditions such that the dispersive shallow water equations, which is an ideal fluid model, can be properly used: K_w is smaller than one (so that no separation must occur) and the incident wave is moderately high (so that nonlinearity plays a role). The solitary wave is supposed to propagate in a channel with a rectangular cross section of half width 19.2 and of length 70. The circular cylinder has a diameter of 4 and its axis is located in (0, 0). The channel is large enough so that, for a certain time after the interaction between the wave and the cylinder, the walls of the channel do not affect the flow. The initial surface of the wave has its crest located in $x = -10$ with a height equal to 0.3; the wave starts traveling in the positive x direction at the initial time $t = 0$.

The computational mesh is composed by 17,119 nodes; the mesh is unstructured, with a local refinement in the region surrounding the cylinder. The side lenght of the triangles of the mesh ranges between 0.15 and 0.5. The mesh has been tuned in such a way to ensure a maximum side lenght of 0.5, corresponding to the minimum spatial step that was observed to be necessary for accurate computations in 1D. The smaller triangles are located around the cylinder. Figure 8 shows the details of the computational mesh in the region around the cylinder.

A time step of $\Delta t = 0.25$ has been used in the computation, and the simulation has been carried out until $t = 28$, corresponding to 112 time steps. The solution of the linear system of $6N$ equations has been obtained iteratively by a bi-conjugate gradient algorithm with diagonal preconditioning. The value of the parameter θ has been posed equal to 3, corresponding to a slightly dissipative scheme.

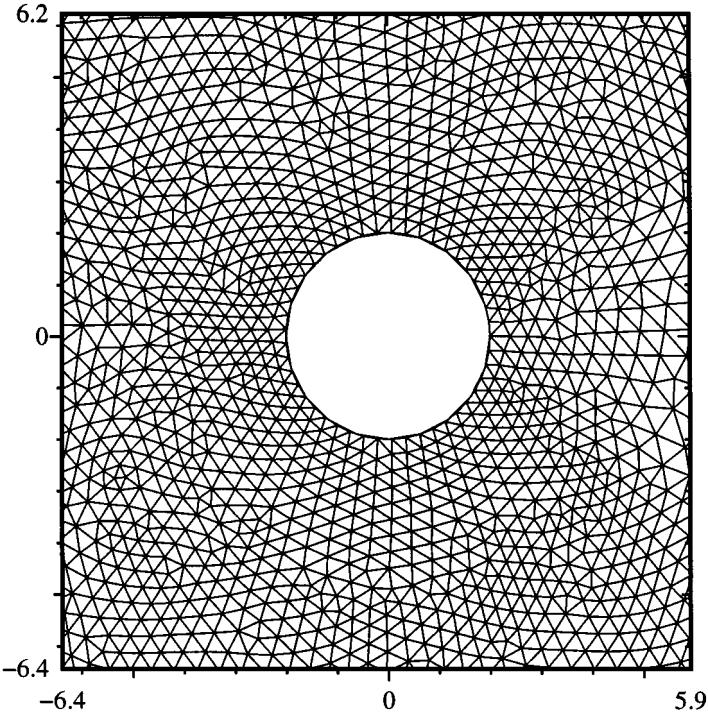

FIG. 8. Solitary wave on a cylinder, details of the computational mesh around the cylinder.

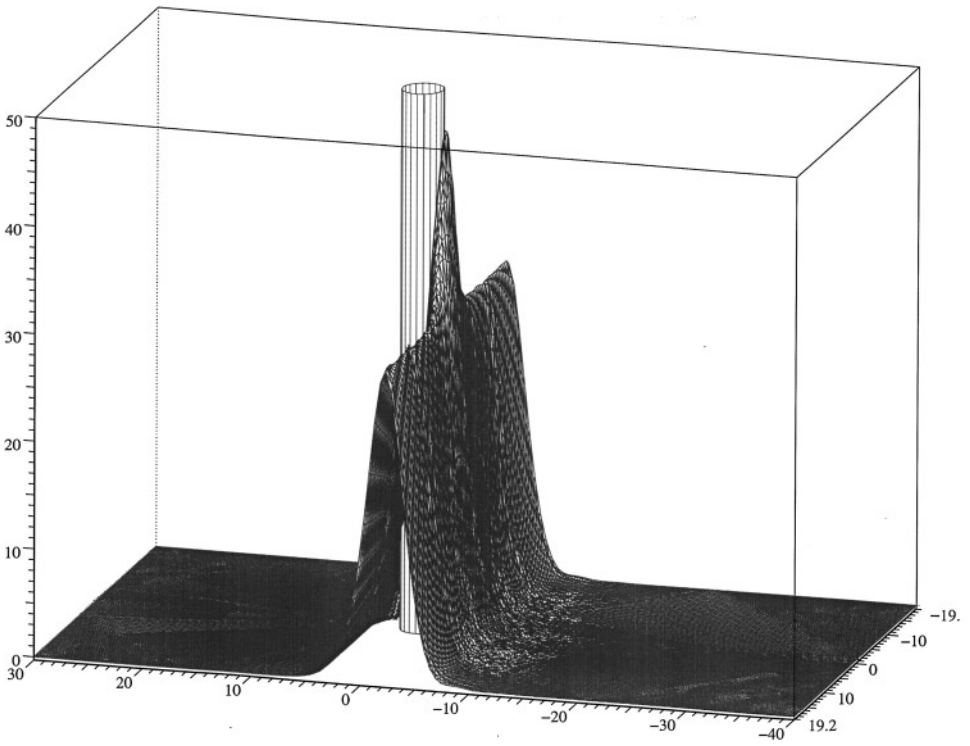

FIG. 9. Solitary wave on a cylinder, elevation of the water at time $t = 7$.

Figures 9–12 show the elevation of the water at different times of the simulation. The vertical scale has been magnified 100 times. At $t = 7$ (Fig. 9) the wave is just running up the cylinder, reaching a maximum height of 0.47. No wave reflection is yet visible. At $t = 14$ (Fig. 10) the scattering and reflection of the impinging wave are evident: the incident wave has overpassed the cylinder, has lost its original transversal uniformity, and shows two minima of height 0.27, located at a distance from the channel midplane equal to the cylinder radius. At the same time a reflected wave is leaving the cylinder.

As a later time, it can be noticed that the part of the solitary wave which has a lower height, because its propagation has been affected by the presence of the cylinder in the channel, does not suffer from any lag with respect to the rest of the wave (Fig. 11). This remarkable behavior has been noticed also in [31]. Moreover, the impinging solitary wave tends to recover its initial shape as it moves farther and farther from the obstacle.

At $t = 28$ (Fig. 12) the pattern of the water elevation has become more complicated, but two main structures can be observed. Several circular diffracted waves of different height propagate away from the cylinder surface. These kinds of circular belts travel freely from the cylinder, until they are reflected by the side walls, while behind the cylinder they interact with the tail of the back-scattered wave.

8. CONCLUSIONS

In this paper we have introduced a new accurate and (linearly) unconditionally stable finite element scheme of Taylor–Galerkin type for the simulation of nonlinear dispersive water

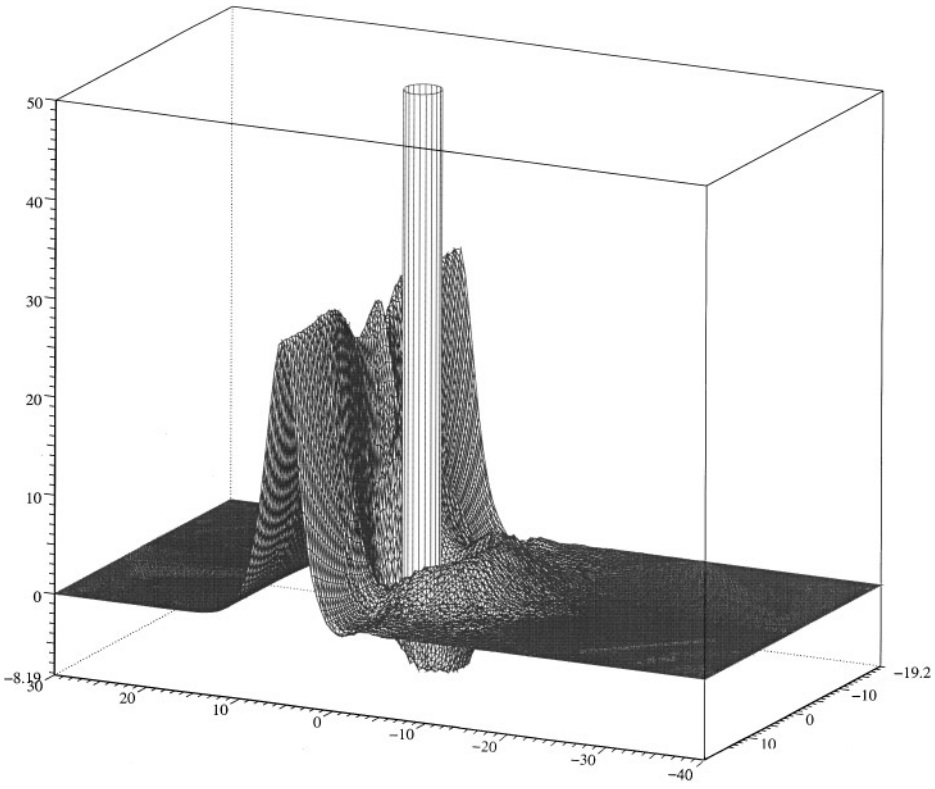

FIG. 10. Solitary wave on a cylinder, elevation of the water at time $t = 14$.

waves. Due to the presence of dispersive terms, the classical Taylor–Galerkin approach had to be revisited and modified accordingly. In fact, the presence of dispersion calls for the introduction of auxiliary variables—the time derivative of the original unknowns—whose space-time discretization is coupled with that of the unknowns of the original dispersive shallow water system. Such an augmentation affects the stability properties of the numerical scheme, making it necessary to choose suitable values for a free parameter of the discretization to ensure stability. The linear stability analysis determines the range of this parameter to guarantee stability and also the value to ensure zero dissipativity, in the sense of Kreiss.

The proposed approach can be used also for dispersive shallow water models different from the classical one. If the operator L defined in (2.8) is linear, nothing changes in the form of the scheme as given by Eqs. (3.17)–(3.18). If L is nonlinear, the derivation of the scheme has to be revisited, case by case, although the underlying philosophy is expected to be applicable effectively.

Admittedly, the Taylor–Galerkin scheme presented here is computationally rather expensive. On the other hand, the scheme is unconditionally stable, zero dissipative, and second order accurate in time. Even more remarkably, the scheme for 1D problems is characterized by a compact stencil, which reveals a major advantage when the scheme is extended to deal with 2D problems: the integrals occurring in the finite element method can be evaluated very easily and the data structure is most simple.

The performance of the numerical scheme has been tested in few examples, showing accuracy and unconditional stability in actual nonlinear calculations. The possibility of

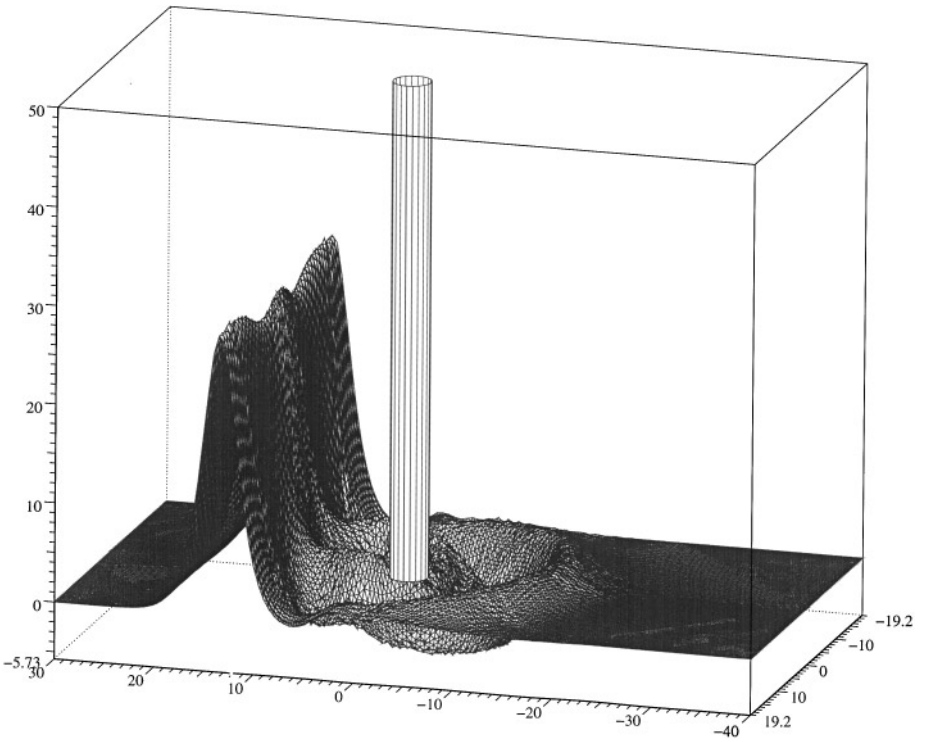

FIG. 11. Solitary wave on a cylinder, elevation of the water at time $t = 21$.

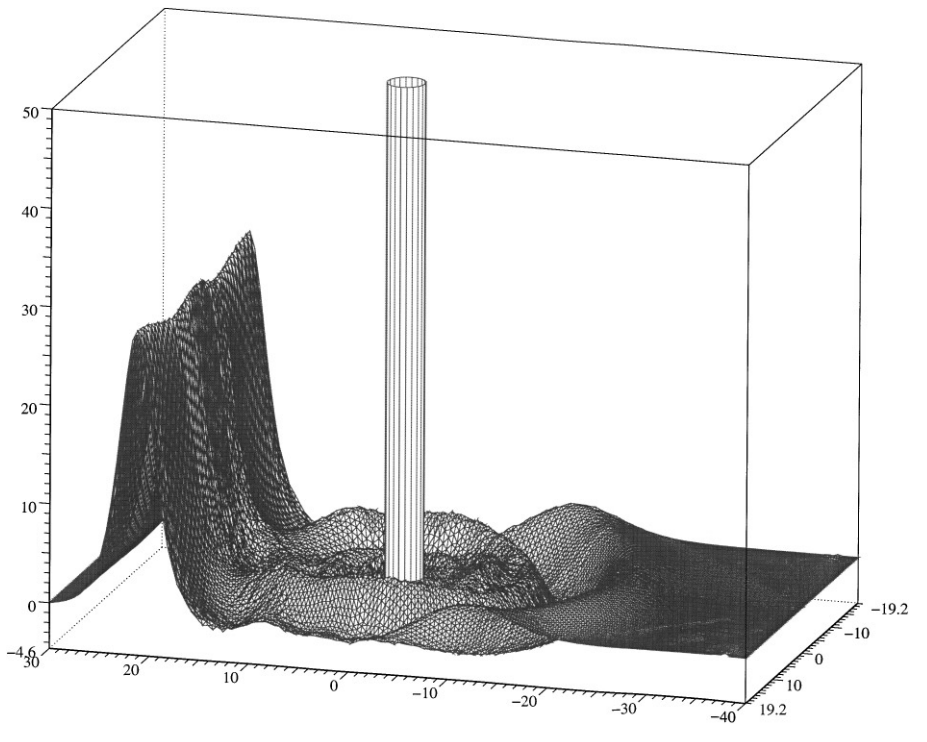

FIG. 12. Solitary wave on a cylinder, elevation of the water at time $t = 28$.

using unstructured triangular meshes ensures a great flexibility to the method, which can be used in arbitrarily complicated domains, including the modeling of small scale coastal circulation.

APPENDIX

Let us look for a class of solutions to problem (2.4), with $H =$ constant, which vanish for $|x| \to \infty$ with its first and second derivative and which are of the type $\mathbf{u} = \mathbf{u}(x - Ut)$, where U is a constant speed to be determined. The solution $\mathbf{u} = (\xi, v)$ is governed by the system of equations

$$\xi_t + v\xi_x + (H + \xi)v_x = 0,$$
$$v_t - \frac{1}{3}H^2 v_{txx} + g\xi_x + vv_x = 0.$$

By introducing the dimensionless variables

$$\zeta = \frac{\xi}{H}, \quad w = \frac{v}{U}, \quad \text{and} \quad \eta = \frac{x - Ut}{H},$$

the solution $(\zeta(\eta), w(\eta))$ satisfies the ordinary differential system

$$-\zeta' + (w\zeta + w)' = 0,$$
$$-w' + \frac{1}{3}w''' + ww' + \frac{gH}{U^2}\zeta' = 0,$$

the prime denoting the differentiation with respect to η, under the boundary conditions $(\zeta, w) \to 0$ as $|\eta| \to \infty$.

The integration of the first equation gives immediately

$$\zeta = \frac{w}{1 - w}$$

since the constant of integration is zero because $(\zeta, w) \to 0$ as $|\eta| \to \infty$. We assume that $w(\eta) < 1, \forall \eta$.

By eliminating ζ in the second equation, we obtain the separate equation

$$\frac{1}{3}w''' - w' + ww' + \frac{gH}{U^2}\left(\frac{w}{1 - w}\right)' = 0,$$

which can be integrated to give

$$\frac{1}{3}w'' = w - \frac{1}{2}w^2 - \frac{gH}{U^2}\frac{w}{1 - w},$$

the new constant of integration being zero since $w \to 0$ and $w'' \to 0$ as $|\eta| \to \infty$. By multiplying this equation by w', a further integration gives

$$(w')^2 = 3w^2 - w^3 + \frac{6gH}{U^2}[w + \ln(1 - w)],$$

the third constant of integration being zero since $w \to 0$ and $w' \to 0$ as $|\eta| \to \infty$. Requiring now that the solution $w(\eta)$ [as $\zeta(\eta)$] has a maximum for $\eta = 0$, i.e.,

$$w'(0) = 0 \quad \text{and} \quad w(0) = w_0,$$

with $w_0 < 1$, we obtain

$$\frac{U^2}{6gH} = \frac{w_0 + \ln(1 - w_0)}{(w_0 - 3)w_0^2}.$$

Note that the right-hand side is always positive for $0 < w_0 < 1$.

In conclusion, assuming $w(\eta)$ is the even function solution to the first order ODE

$$(w')^2 = (3 - w)w^2 - \frac{(3 - w_0)w_0^2}{w_0 + \ln(1 - w_0)}[w + \ln(1 - w)] \tag{A.1}$$

and satisfying the initial condition $w(0) = w_0$, we obtain the following one-parameter family of solutions ($h = \xi + H$, v) to the original system,

$$h(x, t) = \frac{H}{1 - w\big((x - U_{w_0}t)/H\big)},$$
$$v(x, t) = U_{w_0} w\big((x - U_{w_0}t)/H\big),$$

where

$$U_{w_0} = \pm\sqrt{6gH\frac{w_0 + \ln(1 - w_0)}{(w_0 - 3)w_0^2}}. \tag{A.2}$$

ACKNOWLEDGMENT

The authors are sincerely grateful to the reviewers for their constructive comments and remarks that have greatly improved the content and style of the paper.

REFERENCES

1. C. I. Christov and M. G. Velarde, Inelastic interaction of Boussinesq solitons, *Internat. J. Bifur. Chaos* **4**, 1095 (1994).
2. J. Sander and K. Hutter, On the development of the theory of the solitary wave. A historical essay, *Acta Mechanica* **86**, 111 (1991).
3. C. H. Su and C. S. Gardner, Korteweg de Vries equation and generalizations. III. Derivation of the Korteweg de Vries equation and Burgers equation, *J. Math. Phys.* **10**, 536 (1969).
4. D. H. Peregrine, Long waves on a beach, *J. Fluid Mech.* **27**, 815 (1967).
5. O. Nwogu, Alternative form of Boussinesq equations for nearshore wave propagation, *J. Waterway Port Coastal Ocean Engrg.* **119**, 618 (1993).
6. J. M. Witting, A unified model for the evolution of nonlinear water waves, *J. Comput. Phys.* **56**, 203 (1984).
7. C. C. Mei, *The Applied Dynamics of Ocean Surface Waves* (World Scientific, Singapore, 1989).
8. G. B. Whitham, *Linear and Non Linear Waves* (Wiley, New York, 1974).
9. D. Ambrosi, Approximation of shallow water equations by Roe's Riemann solver, *Internat. J. Numer. Meth. Fluids* **20**, 157 (1995).

10. D. Ambrosi, S. Corti, V. Pennati, and F. Saleri, Numerical simulation of unsteady flow at Po river delta, *J. Hydraulic Engrg.* **122** (1996).
11. M. B. Abbott, A. D. McCowan, and I. R. Warren, Accuracy of short wave numerical models, *J. Hydraulic Engrg. ASCE* **110**, 1287 (1984).
12. J. S. Antunes Do Carmo, F. J. Seabra Santos, and E. Barthelemy, Surface wave propagation in shallow water: A finite element model, *Internat. J. Numer. Meth. Fluids* **16**, 447 (1993).
13. S. Kato, A. Anju, and M. Kawahara, A finite element study of solitary wave by Boussinesq equation, in *Computational Methods in Water Resources X* (Kluwer, Dordrecht/Norwell, MA, 1994), p. 1067.
14. D. G. Goring and F. Raichlen, Propagation of long waves onto shelf, *J. Waterway Port Coastal Ocean Engrg.* **118**, 43 (1992).
15. K. D. Katopodes and C. T. Wu, Computation of finite amplitude dispersive waves, *J. Waterway Port Coastal Ocean Engrg.* **113**, 327 (1987).
16. J. Donea, A Taylor–Galerkin method for convective transport problems, *Internat. J. Numer. Meth. Engrg.* **20**, 101 (1984).
17. J. Donea, L. Quartapelle, and V. Selmin, An analysis of time discretization in finite element solution of hyperbolic problems, *J. Comput. Phys.* **70**, 463 (1987).
18. J. Donea, S. Giuliani, H. Laval, and L. Quartapelle, Time-accurate solution of advection–diffusion problems by finite elements, *Comput. Meth. Appl. Mech. Engrg.* **45**, 123 (1984).
19. K. W. Morton, Finite element methods for hyperbolic problems, in *Finite Elements in Physics*, edited by R. Gruber, (North Holland, Amsterdam, 1987).
20. D. Ambrosi, A new finite element scheme for the Boussinesq equations, *Math. Models Methods Appl. Sci.* **7**, 193 (1997).
21. M. E. Alexander and J. L. Morris, Galerkin methods applied to some model equations for non-linear dispersive waves, *J. Comput. Phys.* **30**, 428 (1979).
22. P. D. Lax and B. Wendroff, Systems of conservation laws, *Comm. Pure Appl. Math.* **13**, 217 (1960).
23. A. Quarteroni and A. Valli, *Numerical Approximation of Partial Differential Equations* (Springer-Verlag, Berlin/New York, 1994).
24. T. G. Benjamin, J. L. Bona, and J. J. Mahony, Model equation for long waves in nonlinear dispersive systems, *Philos. Trans. Roy. Soc. London* **272**, 47 (1972).
25. C. Hirsch, *Numerical Computation of Internal and External Flows* (Wiley, New York, 1988), Vol. 1.
26. J. L. Bona and M. Chen, A Boussinesq system for two-way propagation of nonlinear dispersive waves, submitted for publication.
27. N. D. Katopodes and M. W. Dingemans, Hamiltonian approach to surface wave propagation, in *Hydrocomp* (IAHR, 1989), p. 137.
28. M. H. Teng and T. Y. Wu, Nonlinear water waves in channels of arbitrary shape, *J. Fluid Mech.* **242**, 211 (1992).
29. R. L. Herman and C. J. Knickerbocker, Numerically induced phase shift in the KdV soliton, *J. Comput. Phys.* **104**, 50 (1993).
30. R. M. Mirie and C. H. Su, Collision between two solitary waves. Part 2. A numerical study, *J. Fluid Mech.* **115**, 475 (1982).
31. K. H. Wang, T. Y. Wu, and G. T. Yates, Three dimensional scattering of solitary waves by vertical cylinder, *J. Waterway Port Coastal Ocean Engrg.* **118**, 551 (1992).